Metallophysics and Advanced Technologies
Металофіз. новітні технол.
Metallofiz. Noveishie Tekhnol.
2025, vol. 47, No. 12, pp. 1281–1293
https://doi.org/10.15407/mfint.47.12.1281
Reprints available directly from the publisher

PACS numbers: 61.72.Hh, 61.72.Lk, 62.20.fg, 62.40.+i, 64.70.kd, 65.40.De, 81.30.Kf

Elasticity at Martensitic Inelastic Behaviour for Industrial NiTi, CuAlMn and Novel High-Entropy TiZrHfCoNiCu Shape-Memory Alloys

Yu. M. Koval, V. S. Filatova, V. V. Odnosum, O. A. Shcheretskyi*, and G. S. Firstov

G. V. Kurdyumov Institute for Metal Physics, N.A.S. of Ukraine,
36 Academician Vernadsky Blvd.,
UA-03142 Kyiv, Ukraine
**Physico-Technological Institute of Metals and Alloys, N.A.S. of Ukraine,*
34/1 Academician Vernadsky Blvd.,
UA-03142 Kyiv, Ukraine

Elastic properties of shape-memory alloys are of great importance because, among other factors, they determine movement of dislocations and thermoelastic phase-equilibrium phenomenon. This paper is concerned with the consideration of the elastic-modulus evolution at temperature-induced martensitic transformation compared with such at the shape-memory temperature cycle for NiTi, CuAlMn and TiZrHfCoNiCu shape-memory alloys.

Key words: martensitic transformation, elastic modulus, shape memory, internal friction, shape-memory alloys.

Пружні властивості стопів з пам'яттю форми є важливими, оскільки, серед інших чинників, вони визначають рух дислокацій та явище термопружньої фазової рівноваги. Ця стаття стосується розгляду еволюції модуля пружности за температурно-індукованого мартенситного перетворення порівняно з такою за температурного циклу пам'яті форми для стопів з пам'яттю форми NiTi, CuAlMn і TiZrHfCoNiCu.

Corresponding author: Georgiy Serhiyovych Firstov
E-mail: yuri.firstov@gmail.com

Citation: Yu. M. Koval, V. S. Filatova, V. V. Odnosum, O. A. Shcheretskyi, and G. S. Firstov, Elasticity at Martensitic Inelastic Behaviour for Industrial NiTi, CuAlMn and Novel High-Entropy TiZrHfCoNiCu Shape-Memory Alloys, *Metallofiz. Noveishie Tekhnol.*, **47**, No. 12: 1281–1293 (2025). DOI: 10.15407/mfint.47.12.1281

Ключові слова: мартенситне перетворення, модуль пружности, пам'ять форми, внутрішнє тертя, стопи з пам'яттю форми.

(Received 10 October, 2025; in final version, 5 December, 2025)

1. INTRODUCTION

NiTi and Cu-based shape-memory alloys are those that belong to the group of industrial shape-memory alloys. They undergo thermoelastic martensitic transformation and because of that exhibit quite good characteristics of shape memory and related phenomena [1]. Novel high-entropy TiZrHfCoNiCu shape-memory alloys [2–4] were developed because of the need to overcome difficulties with industrial ones (narrow temperature interval, functional fatigue). The application of the high-entropy concept using NiTi as a prototype resulted in a first successful attempt in the TiZrHfCoNiCu alloy system with a martensitic transformation accompanied by a shape-memory effect in a wide temperature range with the suppression of all the fatigue effects due to the two-fold increase in yield strength ensured by the multi-component design. The aim of the present paper is to compare elastic modulus behaviour for alloys mentioned above and to show differences that are quite important for thermoelastic phase equilibrium and dislocations movement. The latter causes irreversibility, when full dislocations are involved and catastrophic for shape-memory plastic deformation accompanies reversible martensitic deformation. On the other hand, with respect to thermoelastic phase equilibrium phenomenon, twinning and martensitic transformation are known to propagate with the help of partial dislocations or so-called twinning dislocation and transformation dislocation. The concepts of twinning and transformation dislocation were developed quite some time ago (see traces of that in the work of Seeger [5] or Van Bueren monograph [6], *etc*.) and are still used (for transformation dislocation with respect to martensite one might look into [7], for example). One way or another, elastic modulus temperature evolution in comparison with shape memory and internal friction might give additional information on reversible and irreversible processes at external stress-free temperature induced martensitic transformation and how external stress influences them with respect to the movement of transformational and twinning dislocations.

2. EXPERIMENTAL

Ni–50 at.% Ti alloy and Ti–16.67 at.% Zr–16.67 at.% Hf–10 at.%. Co–20 at.% Ni–20 at.% Cu alloy were arc-melted and remelted 6 times in a pre-gettered argon atmosphere. Cu–25 at.% Al–4.4 at.% Mn alloy

was induction melted and cast into room temperature ceramic mould. After casting, Cu–25 at.% Al–4.4 at.% Mn alloy was annealed at 1173 K for 30 minutes and quenched into water. These three alloys compositions were chosen because of the similar martensitic transformation temperature interval. Shape-memory behaviour and internal friction changes together with elastic modulus temperature dependencies in 110–440 K temperature interval were obtained in 3-point bending on 22×2×(0.4–0.5) mm plate like specimens (setup with 20 mm distance between nodes; oscillating frequency 5 Hz; heating-cooling rate 5 K/min) using Netzsch 242C Dynamic Mechanical Analyzer (DMA) and Proteus software. In the present case of 3 point bending the deformation was calculated according to the following formula $\varepsilon = [4h(dL)/(l^2 + (dL)^2)] \times 100$, where h is plate thickness, l is distance between nodes (all in mm) and dL is deflection (μm). To measure shape-memory behaviour with the help of DMA, the experiment was set to apply static load well above the temperature range of the martensitic transformation (loaded after heating up to 440 K). Then loaded samples under the bending stress (static 40 MPa for NiTi and CuAlMn, 100 MPa dynamic and 300 MPa static for TiZrHfCoNiCu) were cooled down to 110 K and subsequently heated up back to 440 K and the deflection in 3-point bending versus temperature was observed for them. To determine elastic modulus and internal friction (loss factor) the dynamic load of oscillating force was applied. In the case of major static load, the dynamic oscillating one was applied too with a value of about 10% of the static to ensure proper oscillations under the static load. Proteus software calculates elastic modulus as $|E| = E' + iE''$, where E' is storage modulus and E'' is loss modulus. Storage modulus E' represents the elastic, recoverable energy stored in the material, while loss modulus E'' represents the viscous, energy-dissipating portion. Loss factor, therefore, is obtained as $\mathrm{tg}\delta = E''/E' \approx Q^{-1} = \Delta W/(2\pi W)$, where ΔW is the energy (generally converted into heat) absorbed after loading and unloading and W is the applied energy during loading.

3. RESULTS AND DISCUSSION

First, let us consider the functional and elastic behaviour for NiTi shape-memory alloy. Figure 1 represents comparison of shape memory and corresponding internal friction upon first cooling-heating cycle.

According to Figure 1, the NiTi sample accumulated 0.5% of martensitic strain under the constant stress of 40 MPa in the temperature interval of the forward martensitic transformation ($Ms = 340$ K, $Mf = 260$ K). In this interval a broad peak (full width at half maximum (FWHM) is 25 K) of the loss factor arises reaching almost 0.08 value. After cooling to 215 K subsequent heating takes place. Upon heating, almost complete shape recovery ($K_{\mathrm{SME}} = 96\%$) takes place in the reverse

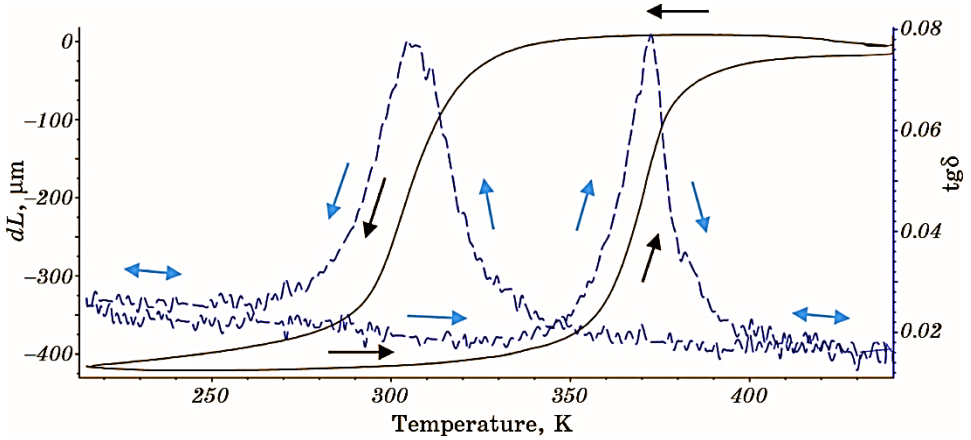

Fig. 1. Deflection in 3-point bending (dL is solid line) and corresponding loss factor tgδ (dashed line) *vs.* temperature measured in Netzsch 242C DMA under constant static stress of 40 MPa for NiTi. Deflection of −410 μm corresponds to 0.5% of accumulated martensitic strain.

martensitic-transformation temperature interval ($As = 330$ K, $Af = 410$ K). In this interval (same in width to the forward one—80 K) internal friction peak arises with the same height of almost 0.08, but with twice narrower $FWHM = 13$ K. Comparing with classic data on internal friction for NiTi external stress-free temperature induced martensitic transformation [8–11], which is around the value of 0.03–0.05 at peaks at 1 Hz, it can be concluded that loss factor shows just peaks that contain two contributions, namely, 'transient' and 'non-transient'; the former exists only during cooling or heating ($\dot{T} \neq 0$ K), depends upon the transformation kinetics and proportional to the volume fraction, which is transformed, while the latter is related to phase transformation mechanism, independent of the transformation rate, such as the movement of parent/martensite or martensite/martensite interfaces according to [11]. Actually, movement of the parent/martensite interface is ensured by the movement of the transformational dislocation, while internal martensite twinning known as lattice invariant shear is related to the movement of the twinning dislocation.

At the same time, the 'intrinsic' loss factor contribution (again according to [11]), that exists in both parent $B2$ and $B19'$ martensitic phases and strongly depends upon microstructural properties, is very small in $B2$ austenite (temperature interval 400–440 K, Fig. 1) and is only slightly higher in martensite state (215–260 K, Fig. 1) indicating that formation under external stress of the oriented martensite crystals that resulted in shape memory and internal friction shown in Fig. 1 lead to the stationary martensite microstructure without any signs of intervariant martensite boundaries mobility. Results of Refs. [8, 9]

clearly show high internal friction in NiTi martensite state for external stress-free experiments indicating that in this case intervariant martensite boundaries are mobile. It should be also noted that broader loss factor peak for forward transformation compared to reverse (FWHM twice wider) indicates more intensive parent/martensite and martensite/martensite interfaces movement at the formation of $B19'$ martensitic crystals, while their disappearance on reverse transformation is characterized by twice weaker movement of the interfaces in NiTi shape-memory alloy.

Figure 2 shows storage modulus *vs.* temperature against the background of shape-memory thermal cycle. Qualitatively, the results of Refs. [8, 9] show the elastic modulus behaviour similar to the one in Fig. 2. *Ms* temperature (340 K) corresponds to the change of slope for storage modulus temperature dependence on cooling. The same can be observed for *Mf* temperature (260 K) on cooling and for *Af* temperature (410 K) on heating. *As* temperature cannot be deduced from storage modulus behaviour as there is no change of its slope in the vicinity of *As* from deflection temperature dependence. Storage modulus minima correspond well to the peaks of the loss factor from Fig. 1. It should be also noted that the minimum in the middle of the forward martensitic transformation on cooling is deeper compared with the minimum in the middle of reverse martensitic transformation on subsequent heating (Fig. 2) implying that lattice softening during forward martensitic transformation is more significant for NiTi.

Results shown in Figure 3 from the work [12] represent the temperature dependencies of elastic constants measured by resonant ultrasound spectroscopy upon cooling and subsequent heating through the

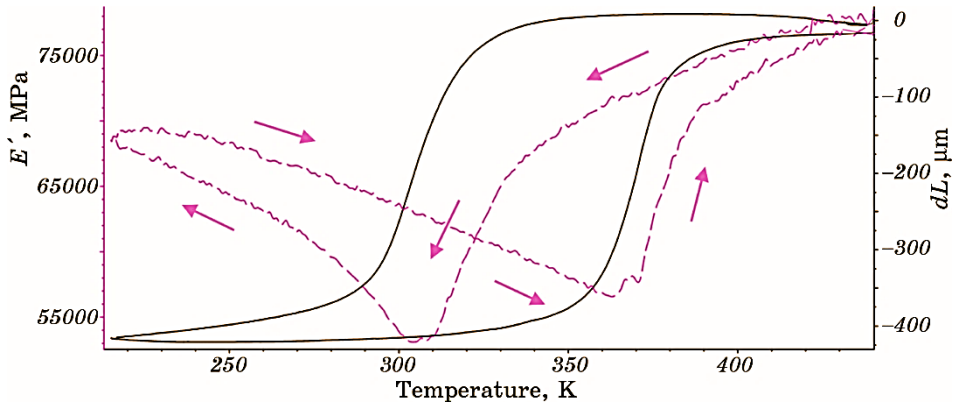

Fig. 2. Deflection in 3-point bending (dL is solid line) and storage modulus E' (dashed line) *vs.* temperature measured in Netzsch 242C DMA under constant static stress of 40 MPa for NiTi. Deflection of −410 μm corresponds to 0.5% accumulated martensitic strain.

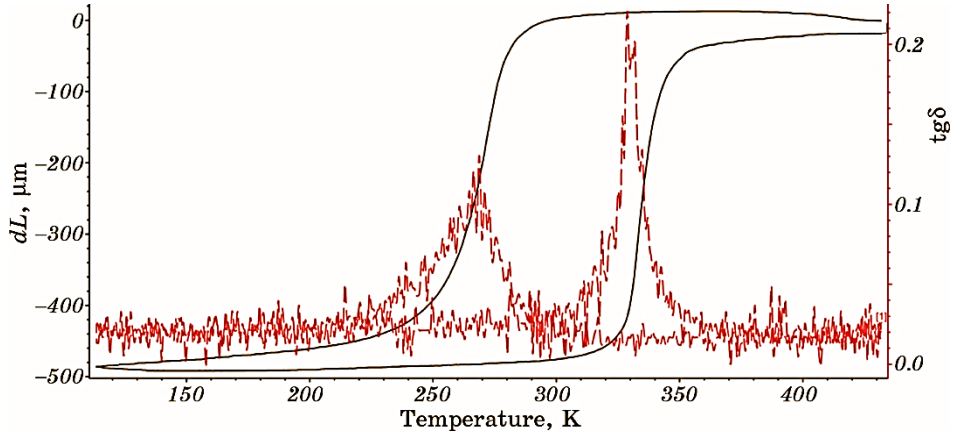

Fig. 3. Deflection in 3-point bending (dL is solid line) and corresponding loss factor tgδ (dashed line) *vs.* temperature measured in Netzsch 242C DMA under constant static stress of 40 MPa for CuAlMn. Deflection of −500 μm corresponds to 1% of accumulated martensitic strain.

martensitic transformation in NiTi single crystalline specimen. C_{44} temperature behaviour (Fig. 3, *b* [12]) is qualitatively the same as storage modulus behaviour (Fig. 2 of this work) implying that it is dominated by the C_{44} contribution and in the present polycrystalline $B2$ NiTi C_{44} principal shear modulus is at play corresponding to shear on a {001} plane, independent of the direction of shear within that plane.

Now, let us consider how the functional and elastic behaviour *vs.* temperature will look like for Cu–Al–Mn shape-memory alloy, where $L2_1$ austenite undergoes martensitic transformation into the γ_1' orthorhombic martensite. Figure 3 shows comparison of shape memory and corresponding internal friction upon first cooling-heating cycle involving $L2_1 \leftrightarrow \gamma_1'$ thermally induced martensitic transformation with external static load equivalent to the stress of 40 MPa.

According to Figure 3, the CuAlMn sample accumulated 1% of martensitic strain under the constant stress of 40 MPa in the temperature interval of the forward martensitic transformation ($Ms = 290$ K, $Mf = 230$ K). In this interval a peak of the loss factor rises, reaching 0.12 value. After cooling to 115 K subsequent heating takes place. Upon heating, almost complete shape recovery ($K_{SME} = 97\%$) takes place in the reverse martensitic transformation temperature interval ($As = 300$ K, $Af = 360$ K). In this interval, internal-friction peak arises with the height of 0.23. Comparing with the data on internal friction for CuAlMn external stress-free temperature induced martensitic transformation [8–11], which is around the value of 0.09–0.1 at peaks at 1 Hz, it can be concluded that loss factor shows just peaks that contain two contributions, similarly to NiTi (Fig. 1), 'transient' and 'non-

transient'. At the same time, the 'intrinsic' loss factor contribution that exists in both parent $L2_1$ and γ_1' martensitic phases is small (0.02–0.03, Fig. 3) indicating that formation under external stress of the oriented martensite crystals that resulted in shape memory and internal friction shown in Fig. 3 lead to the stationary martensite microstructure without any signs of intervariant martensite boundaries mobility similarly again to the case of NiTi shown in Fig. 1. Results of [13, 14] for CuAlMns alloy show high internal friction in martensite state for external stress-free experiments indicating that in this case intervariant martensite boundaries are mobile. In particular [14], high internal friction in martensite has been detected only for small grain size, while martensite in big grains does not show any signs of the intervariant mobility having the same small internal friction value as in austenite state similarly to the results in Fig. 3. It should be also noted that higher loss factor peak for reverse transformation compared to forward indicates contrary to the case of NiTi that more intensive parent/martensite and martensite/martensite interfaces movement takes place at the disappearance of γ_1' martensitic crystals, while on forward transformation there is weaker movement of the interfaces in CuAlMn shape-memory alloy. Comparison of the internal friction between NiTi (Fig. 1) and CuAlMn (Fig. 3) shows that in a latter case it is much stronger with an emphasis on the reverse martensitic transformation.

Figure 4 shows storage modulus *vs.* temperature against the background of shape-memory thermal cycle in CuAlMn. Qualitatively, the results of [13, 14] show the elastic modulus behaviour similar to the one in Fig. 4 although there are some differences as well. In particular,

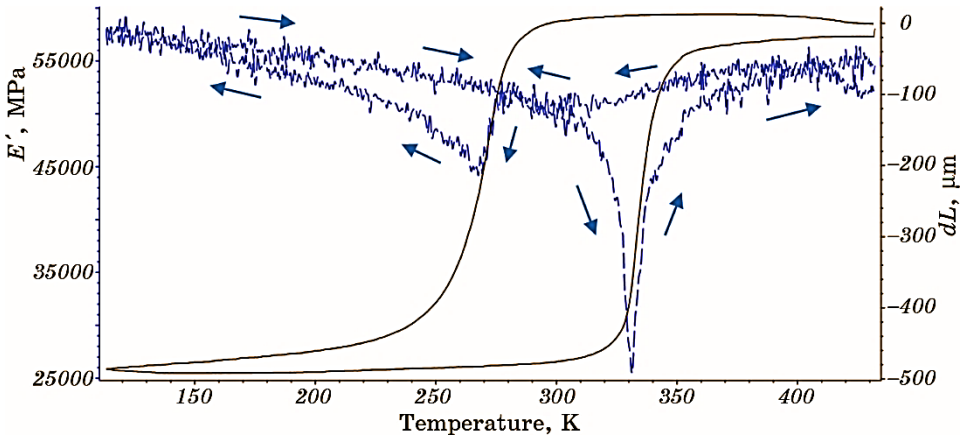

Fig. 4. Deflection in 3-point bending (dL is solid line) and storage modulus E' (dashed line) *vs.* temperature measured in Netzsch 242C DMA under constant static stress of 40 MPa for CuAlMn. Deflection of –500 μm corresponds to 1% accumulated martensitic strain.

Ms temperature (290 K) does not correspond to the change of slope for storage modulus temperature dependence on cooling. At 290 K on cooling storage, modulus tends to grow a bit until it sharply decreases at 275 K. Other characteristic temperatures of martensitic transformation fit for change in deflection and storage modulus (Fig. 4). Storage modulus minima correspond well to the peaks of the loss factor from Fig. 3. It should be also noted that, similarly to the results of [14], the minimum in the middle of the reverse martensitic transformation on cooling is deeper compared with the minimum in the middle of forward martensitic transformation on subsequent heating (Fig. 4) implying that lattice softening during reverse martensitic transformation is more significant contrary to NiTi (Fig. 2).

Results shown in Figure 1 from the work [13] represent the temperature dependences of elastic modulus measured by DMA upon cooling and subsequent heating through the martensitic transformation in CuAlMn polycrystalline wire. Elastic modulus behaviour (Fig. 1 [13]) is qualitatively the same as storage modulus behaviour (Fig. 4 of this work) in the sense that it represents two temperature dependencies with minima implying that similarly to NiTi it is dominated by the C_{44} contribution. Still, the short temperature interval between 275 K and 290 K on cooling (Fig. 4) represents weak growth and, therefore, a possibility of the dominant C' shear modulus (it is derived from a different type of volume preserving shear strain) at this earlier stage of the forward $L2_1 \rightarrow \gamma_1'$ transformation under constant external stress. Still, after the cooling below 275 K and upon subsequent heating in the present polycrystalline CuAlMn C_{44} principal shear modulus is at play corresponding to shear on a {001} plane, independent of the direction of shear within that plane.

Eventually, we arrived at the consideration of the functional and elastic behaviour for the novel TiZrHfCoNiCu high-entropy shape-memory alloy that, as was mentioned above, has been designed using NiTi as a prototype. One might expect some general similarity with NiTi behaviours. Let us check whether it is true for stress-free $B2 \leftrightarrow B19'$ type martensitic transformation in this multicomponent intermetallic, although both $B2$ and $B19'$ phases are triclinically distorted, which is the origin for outstanding double increase in yield strength, for instance.

Figure 5 shows that for $(TiZrHf)_{50}Co_{10}Ni_{20}Cu_{20}$ multicomponent $B2$ distorted intermetallic compound that undergoes martensitic transformation with $B19'$ distorted phase as a product. As the deflection in this case is not influenced by external stress, the deflection hysteresis loop in Fig. 5 represents the volume change, which is negative and is of 0.17%. Loss factor peaks correspond well with deflection slope changes that correspond to characteristic temperatures of martensitic transformation ($Ms = 290$ K, $Mf = 190$ K, $As = 220$ K, $Af = 360$ K). It can be also

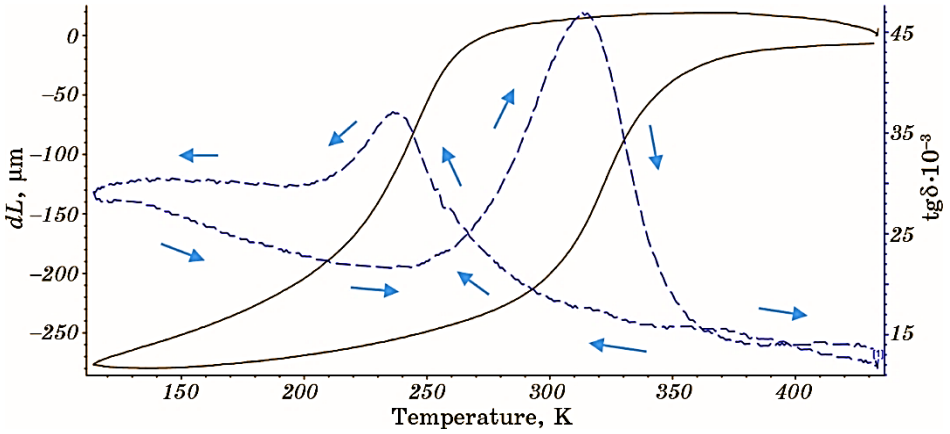

Fig. 5. Deflection in 3-point bending (dL is solid line) and corresponding loss factor tgδ (dashed line) under dynamic stress of 100 MPa *vs.* temperature measured in Netzsch 242C DMA for $(TiZrHf)_{50}Co_{10}Ni_{20}Cu_{20}$. Deflection of −280 μm corresponds to 0.17% of volume change.

seen that internal friction is relatively high in martensite, implying that intervariant martensite boundaries are mobile enough. Loss factor peak upon reverse transformation is almost twice as high as for the forward one. It means that contrary to the case of NiTi the more intensive parent/martensite and martensite/martensite interfaces movement takes place at the disappearance of $B19'$ martensitic crystals, while on forward transformation there is weaker movement of the interfaces in $(TiZrHf)_{50}Co_{10}Ni_{20}Cu_{20}$ multicomponent intermetallic compound.

Figure 6 represents corresponding elastic behaviour against the background of the volume change hysteresis loop in $(TiZrHf)_{50}Co_{10}Ni_{20}Cu_{20}$.

Figure 6 shows storage modulus *vs.* temperature against the background of stress-free volume change hysteresis loop in $(TiZrHf)_{50}Co_{10}Ni_{20}Cu_{20}$. On cooling storage, modulus decreases slightly in pre-martensitic temperature interval, while, at Ms temperature, it decreases sharply and passes through a minimum in the temperature interval of the forward transformation. Then, it significantly growing up to a value of 76 GPa at 115 K after passing a minimum without visible critical point that might correspond to Mf. The same happens upon subsequent heating when it is difficult to define As from storage modulus. Af temperature fits the one of deflection in Fig. 6. Analogously to NiTi, it might then be supposed that in the case of distorted cubic $B2$ structure C_{44} contribution still dominates elastic modulus temperature dependencies and its being a one of the principal shear moduli for cubic structure still corresponding to shear on a {001} plane, independent of the direction of shear within that plane.

Now, let us consider how external stress will influence functional

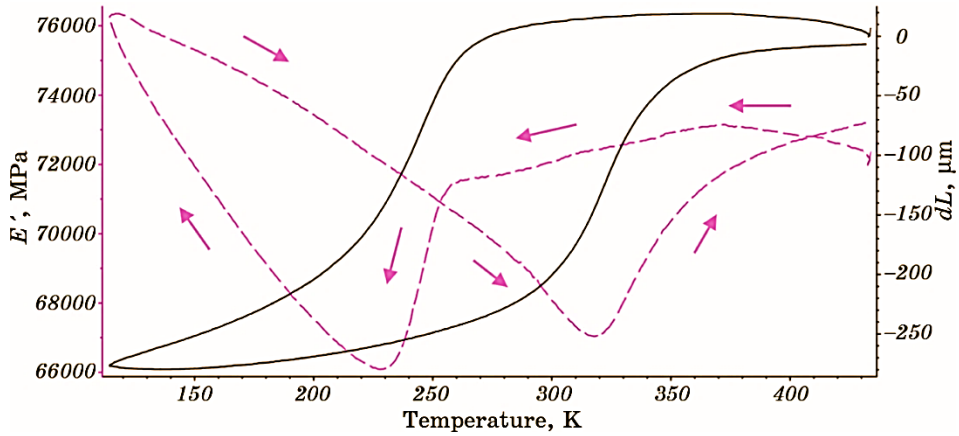

Fig. 6. Deflection in 3-point bending (*dL* is solid line) and storage modulus *E′* (dashed line) under dynamic stress of 100 MPa *vs.* temperature measured in Netzsch 242C DMA for $(TiZrHf)_{50}Co_{10}Ni_{20}Cu_{20}$. Deflection of −280 μm corresponds to 0.17% of volume change.

and elastic behaviour *vs.* temperature for $(TiZrHf)_{50}Co_{10}Ni_{20}Cu_{20}$ multicomponent intermetallic compound.

Figure 7 shows that the $(TiZrHf)_{50}Co_{10}Ni_{20}Cu_{20}$ sample accumulated 0.8% of martensitic strain under the constant stress of 300 MPa in the temperature interval of the forward martensitic transformation ($Ms = 280$ K, $Mf = 170$ K). In this interval, a peak of the loss factor arises reaching value 0.08. After cooling to 115 K subsequent heating

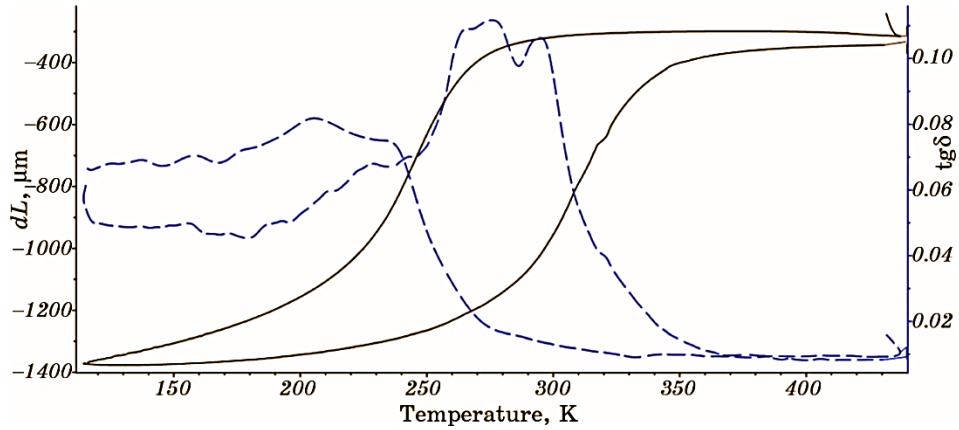

Fig. 7. Deflection in 3-point bending (*dL* is solid line) and corresponding loss factor tgδ (dashed line) *vs.* temperature measured in Netzsch 242C DMA under constant static stress of 300 MPa for $(TiZrHf)_{50}Co_{10}Ni_{20}Cu_{20}$. Deflection of −1056 μm corresponds to 0.8% of accumulated martensitic strain.

takes place. Upon heating, almost complete shape recovery ($K_{SME} = 98\%$) takes place in the reverse martensitic transformation temperature interval ($As = 250$ K, $Af = 350$ K). In this interval, internal friction peak arises with the height of 0.11. Comparing with the data on internal friction for $(TiZrHf)_{50}Co_{10}Ni_{20}Cu_{20}$ external stress-free temperature induced martensitic transformation (Fig. 5), which is around the value of 0.03–0.45 at peaks, it can be concluded that loss factor shows peaks that contain two contributions, similarly to NiTi (Fig. 1), 'transient' and 'non-transient'. At the same time, the 'intrinsic' loss factor contribution that exists in parent $B2$ phase is relatively small but in martensitic state it is high (0.05–0.07, Fig. 7) indicating that formation under external stress of the oriented martensite crystals that resulted in shape memory and internal friction shown in Fig. 7 lead to the martensite microstructure with definite signs of intervariant martensite boundaries mobility. It should be also noted that higher loss factor peak for reverse transformation compared to forward indicates contrary to the case of NiTi that more intensive parent/martensite and martensite/martensite interfaces movement takes place at the disappearance of $B19'$ martensitic crystals, while on forward transformation there is weaker movement of the interfaces in $(TiZrHf)_{50}Co_{10}Ni_{20}Cu_{20}$ shape-memory alloy.

Figure 8 shows storage modulus *vs.* temperature against the background of shape-memory thermal cycle. It can be seen that upon cooling at the earlier stage of the forward transformation storage modulus seemed to start a decrease in 250–290 K temperature interval. Yet, after reaching 250 K on cooling situation changed drastically as storage

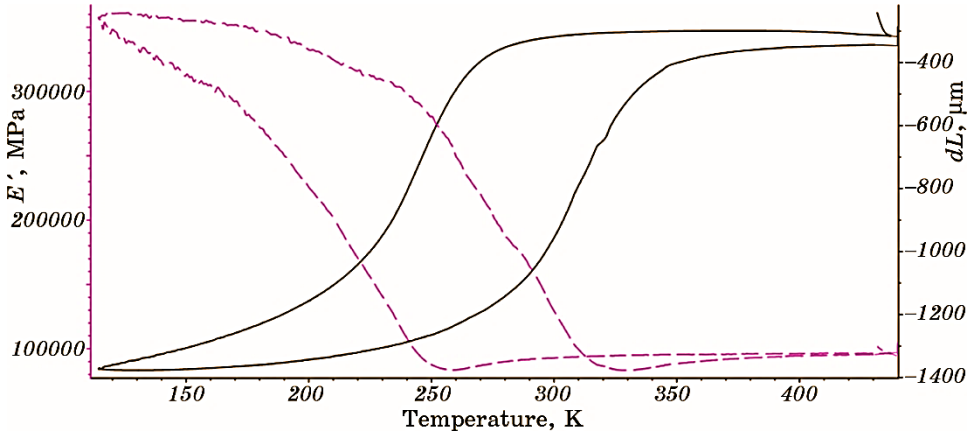

Fig. 8. Deflection in 3-point bending (dL is solid line) and storage modulus E' (dashed line) *vs.* temperature measured in Netzsch 242C DMA under constant static stress of 300 MPa for $(TiZrHf)_{50}Co_{10}Ni_{20}Cu_{20}$. Deflection of –1056 μm corresponds to 0.8% of accumulated martensitic strain.

modulus started to increase and reached 350 GPa at 115 K. Subsequent heating exhibited eventual decrease in storage modulus with the temperature hysteresis similar with shape-memory hysteresis loop. Slight minimum in storage modulus prior to Af takes place with hysteresis in respect to small minimum on cooling. Taking into account the results of [12] obtained on single crystalline NiTi, it can thus be supposed that small minimum appeared on cooling at first due to C_{44} principal shear modulus contribution, while after that C' contribution completely dominated storage modulus behaviour corresponding to shear in the (110) plane and the $[1\bar{1}0]$ direction.

4. SUMMARY

In stress free conditions elastic modulus minimum for NiTi is deeper at forward martensitic transformation and is accompanied by corresponding more significant internal friction compared with reverse one implying that lattice softening is more pronounced at martensite formation and the movement of the transformation dislocations is easier in this case. CuAlMn shows behaviour opposite to NiTi; reverse martensitic transformation exhibits deeper elastic modulus minimum and stronger corresponded internal friction implying that lattice softening is more pronounced and transformation dislocations glide easier at martensite disappearance. TiZrHfCoNiCu exhibits elastic modulus behaviour similar to NiTi, while internal friction is similar to CuAlMn meaning that the lattice softening (deeper modulus minimum) is more significant for the martensite formation, while the internal friction associated with transformation dislocations movement is much stronger for the martensite crystals disappearance.

As supposed, while comparing the elastic behaviour under external stress with respect to functional properties changes for NiTi, CuAlMn and TiZrHfCoNiCu polycrystalline shape-memory alloys, that C_{44} contribution dominates elastic modulus behaviour for NiTi and CuAlMn upon shape memory and internal friction and corresponds to shear on a {001} plane, independent of the direction of shear within that plane.

As for TiZrHfCoNiCu, it was supposed that its elastic modulus behaviour upon shape memory and internal friction is dominated by C' contribution that corresponds to shear in the (110) plane and the $[1\bar{1}0]$ direction. Detailed analysis of the directional dependence of elastic stiffness and shear moduli that helped us to put shear constants in correspondence with two principal shear systems might be found in [15] and [16].

There is a competition between two principal shear systems at forward martensitic transformation under external stress for CuAlMn and TiZrHfCoNiCu shape-memory alloys. In CuAlMn, (110) plane and the $[1\bar{1}0]$ principal shear lead at first to stiffening, while at some point {001} plane shear system takes over. On a contrary, in

TiZrHfCoNiCu at the initial stage there is some softening associated with {001} plane shear system, while later on (110) plane and the $[1\bar{1}0]$ direction shear system takes over. Consequences of such competition need to be studied in more detail.

It is possible that supposed change in principal shear at transition from industrial NiTi and CuAlMn to highly distorted TiZrHfCoNiCu high-entropy shape-memory alloys might be the reason for the advanced functional properties of the novel multicomponent materials. It also might indicate that thermoelastic behaviour can be different for TiZrHfCoNiCu high-entropy shape-memory alloys comparing with NiTi and CuAlMn due to the noticed differences in elastic modulus and internal friction correspondence upon forward and reverse martensitic transformation. The more detailed pursuit of these differences will be the subject of our future investigations.

Authors of this work are grateful for the support from the National Academy of Sciences of Ukraine through the grant 0123U101764.

REFERENCES

1. K. Otsuka and C. M. Wayman, *Shape Memory Materials* (Cambridge: Cambridge University Press: 1998).
2. G. S. Firstov, T. A. Kosorukova, Yu. N. Koval, and V. V. Odnosum, *Mater. Today Proc.*, **2**: S499 (2015).
3. G. S. Firstov, T. A. Kosorukova, Y. N. Koval, and P. A. Verhovlyuk, *Shape Memory and Superelasticity*, **1**: 400 (2015).
4. G. S. Firstov, Yu. M. Koval, V. S. Filatova, V. V. Odnosum, G. Gerstein, and H. Maier, *Progress in Physics of Metals*, **24**, No. 4: 819 (2023).
5. A. Seeger, *Int. J. Mater. Research*, **47**, Iss. 9: 653 (1956).
6. H. G. van Bueren, *Imperfections in Crystals* (Amsterdam: North Holland Publishing Co: 1960).
7. H. Heinrich, H. P. Karnthaler, T. Waitz, and G. Kostorz, *Mater. Sci. Eng. A*, **272**, Iss. 1: 238 (1999).
8. R. R. Hasiguti and K. Iwasaki, *J. Appl. Phys.*, **39**: 2182 (1968).
9. S. Spinner and A. G. Rozner, *J. Acoustical Soc. America*, **40**: 1009 (1966).
10. G. Mazzolai, *AIP Advances*, **1**: 040701 (2011).
11. J. Van Humbeeck, J. Stoiber, L. Delaey, and R. Gotthardt, *Int. J. Mater. Research*, **86**: Iss. 3: 176 (1995).
12. L. Bodnárová, M. Janovská, M. Ševčík, M. Frost, L. Kadeřávek, J. Kopeček, H. Seiner, and P. Sedlák, *Shape Memory and Superelasticity*, **11**: 230 (2025).
13. N. Koeda, T. Omori, Y. Sutou, H. Suzuki, M. Wakita, R. Kainuma, and K. Ishida, *Mater. Trans.*, **46**: 118 (2005).
14. Yu. M. Koval, V. V. Odnosum, Vyach. M. Slipchenko, V. S. Filatova, A. S. Filatov, O. A. Shcheretskyi, and G. S. Firstov, *Metallofiz. Noveishie Tekhnol.*, **46**, No. 9: 933 (2024).
15. K. M. Knowles and P. R. Howie, *J. Elasticity*, **120**: 87 (2015).
16. C. Zener, *Elasticity and Anelasticity of Metals* (Chicago: University of Chicago Press: 1948).